

**FINAL REPORT**

**VALIDATION OF THE H-SAF PRECIPITATION  
PRODUCTS OVER BRAZIL USING THE CHUVA  
CAMPAIGN DATASET**

Lia Martins Costa do Amaral

H-SAF Visiting Scientist

HSAF\_CDOP2\_VS17\_02

October, 2017

## **ABSTRACT**

The activities developed in the Visiting Scientist (HSAF\_CDOP2\_VS17\_02) are intended as the integral part of the Federated Activity proposal entitled “Assessment of ground-reference data in Brazil and validation of the H-SAF precipitation products in the perspective of CDOP-3” that is aimed at setting up the framework for the validation of the H-SAF precipitation products on the MSG Full Disk area, being a crucial task of CDOP-3.

Thereby, the goal of the present proposal is to verify the performance of the H-SAF precipitation products H01, H02 and H18 in Brazil in comparison with X Band Radar data collected during CHUVA field campaigns. The validation procedure during entire activity will be made for four different experiments, being them: Fortaleza, Belém, Vale do Paraíba and Manaus.

## LIST OF FIGURES

	<u>Page</u>
Figure 1 - Technical bulletin of synoptical conditions on 13th April, 2011 at 00:00UTC at surface (left) and at 500hPa level (right). .....	11
Figure 2 - RHI (Range Height Indicator) of a meteorological system observed over Fortaleza on 13/04/2011 at 15:05 UTC.....	11
Figure 3 - RHI (Range Height Indicator) of a meteorological system observed over Fortaleza on 25/04/2011 at a) 10:45UTC and b) 11:51UTC. ....	12
Figure 4 – a) CAPPI of 2 km of X-Band Radar at 23:12 UTC on 13/11/2011 localized on UNIVAP site (São José dos Campos city) and b) daily density of electromagnetic pulses in VHF of the LMA network with resolution of 2 km x 2 km. ....	14
Figure 5 – a) CAPPI of 2 km of X Band Radar at 19:30 UTC on 1/12/2011 localized on UNIVAP site (São José dos Campos city) and b) density of electromagnetic pulses in VHF daily of the LMA network with resolution of 2 km x 2 km. ....	15
Figure 6 - Radar X-Band (CAPPI of 2km) of the events which acted on February, 21, a) 08:20 UTC, b) 08:50 UTC, c) 09:10 UTC, d) 13:40 UTC. ....	17
Figure 7 - Radar X-Band (CAPPI of 2km) of the events which acted on February, 25, a) 18:00 UTC, b) 18:40 UTC and RHI at c) 18:36 UTC, d) 18:46 UTC.....	18
Figure 8 - a) Overall quality index radar and b) Rain rate from radar on 21/02/2014 at 12:10UTC. ....	29
Figure 9 – Rain rate from radar uspcaled to the satellite grid (left), H01 rain rate (center) and overall quality index map (right) in Manaus on 21/02/2014 at 12:10 for a) quality index > 0,5, b) quality index > 0,6 and c) quality index > 0,7.....	29
Figure 10 - a) Overall quality index radar on and b) Rain rate from radar on 08/03/2014 at 05:30UTC. .	30
Figure 11 – Rain rate from radar uspcaled to the satellite grid (left), H02 rain rate (center) and overall quality index map (right) in Manaus on 08/03/2014 at 05:30UTC for a) quality index > 0,5, b) quality index > 0,6 and c) quality index > 0,7. ....	31
Figure 12 - a) Overall quality index radar on and b) Rain rate from radar on 08/03/2014 at 05:10UTC. ...	33

Figure 13 – Rain rate from radar uspscaled to the satellite grid (left), H18 rain rate (center) and overall quality index map (right) in Manaus on 08/03/2014 at 05:10 for a) quality index > 0,5, b) quality index > 0,6 and c) quality index > 0,7..... 33

Figure 14 - a) Overall quality index radar on and b) Rain rate from radar on 01/12/2011 at 21:18UTC. ...34

Figure 15 – Rain rate from radar uspscaled to the satellite grid (left), H01 rain rate (center) and overall quality index map (right) in vale do Paraíba on 01/12/2011 at 21:18 for a) quality index > 0,5, b) quality index > 0,6 and c) quality index > 0,7. .... 35

Figure 16 – Rain rate from radar uspscaled to the satellite grid (left), H02 rain rate (center) and overall quality index map (right) on 08/12/2011 at 18:06 for a) quality index > 0,5, b) quality index > 0,6 and c) quality index > 0,7..... 36

## LIST OF TABLES

	<u>Page</u>
Table 1 – Campaigns and periods of each CHUVA field experiments. ....	4
Table 2 – Precipitating events selected from Fortaleza Campaign. ....	10
Table 3 – Precipitating events selected from Vale do Paraíba Campaign. ....	13
Table 4 – Precipitating events selected from Manaus Campaigns. ....	16
Table 5 - Satellite sensors features and technical informations relative of each algorithm. ....	19
Table 6 – List of continuous statistical scores. ....	21
Table 7 - Multicategory statistical scores. ....	21
Table 8 – Continuous statistical scores for H01 for Manaus, with 905, 672 and 406 pixels pixels for the respective threshold of quality index (QI) (0.5, 0.6, 0.7).. ....	22
Table 9 – Multicategory statistical scores for H01 for Manaus with 7090, 5108 and 3149 pixels for the respective threshold of quality index (QI) (0.5, 0.6, 0.7).. ....	23
Table 10 – Continuous statistical scores for H02 for Manaus with 1085, 907 and 631 pixels for the respective threshold of quality index (QI) (0.5, 0.6, 0.7). ....	24
Table 11 – Multicategory statistical scores for H02 for Manaus with 3757, 2986 and 1889 pixels for the respective threshold of quality index (QI) (0.5, 0.6, 0.7).. ....	24
Table 12 – Continuous statistical scores for H18 for Manaus with 227, 198 and 140 pixels for the respective threshold of quality index (QI) (0.5, 0.6, 0.7).. ....	25
Table 13 – Multicategory statistical scores for H18 for Manaus with 3757, 2986 and 1889 pixels for the respective threshold of quality index (QI) (0.5, 0.6, 0.7). ....	25
Table 14 – Continuous statistical scores for H01 for Vale do Paraíba with 368, 287 and 181 pixels for the respective threshold of quality index (QI) (0.5, 0.6, 0.7) ....	26
Table 15– Multicategory statistical scores for H01 for Vale do Paraíba with 3569, 3197 and 2420 pixels for the respective threshold of quality index (QI) (0.5, 0.6, 0.7). ....	26
Table 16 – Continuous statistical scores for H02 for Vale do Paraíba with 187, 175 and 124 pixels for the respective threshold of quality index (QI) (0.5, 0.6, 0.7). ....	27

Table 17 – Multicategory statistical scores for H02 for Vale do Paraíba with 1445, 1320 and 991 pixels  
for the respective threshold of quality index (QI) (0.5, 0.6, 0.7).....27

## SUMMARY

	<b><u>Page</u></b>
1. INTRODUCTION.....	1
2.THE CHUVA PROJECT .....	3
3. GROUND-BASED REFERENCE: METEOR 50-DX .....	4
4. SATELLITE PRODUCTS .....	6
4.1 H01 – Cloud Dynamics Radiation Database (CDRD) for the conically scanning SSMIS radiometers .	6
4.2 H02 - Passive Microwave Neural Network Precipitation Retrieval (PNPR) for AMSU and MHS cross-track radiometers .....	7
4.3 H18 - Passive Microwave Neural Network Precipitation Retrieval (PNPR) for ATMS cross-track radiometer .....	8
5.1 TASK 1: Selection and preparation of CHUVA Dataset.....	9
5.1.1 Fortaleza Campaign.....	9
5.1.2 Vale do Paraíba Campaign .....	12
5.1.3 Manaus Campaign .....	16
5.2 TASK 2: Satellite dataset generation.....	18
5.3 TASK 3: Application of the Common Validation Code.....	19
6. RESULTS 21	
6.1 Statistical evaluation.....	21
6.2 Pixel by pixel analysis .....	28
7. CONSIDERATIONS AND CONCLUSIONS: .....	37
8. REFERENCES.....	39

## 1. INTRODUCTION

Several efforts to quantify the characteristics of uncertainties (random components and systematic errors) associated to satellite precipitation estimates have been carried out. One example is the CHUVA Project (Cloud processes of the main precipitation systems in Brazil: A contribution to cloud resolving modeling and to the GPM [Global Precipitation Measurement]), which had as main goal to collect information on the cloud processes originated from the main precipitating systems in six different regions in Brazil during specific periods between the years of 2011 and 2014.

It's worth remembering that Brazil has an area of 8.5 million square kilometers and lies primarily south of the equator (and within the tropics), being ideally situated for studies of tropical continental convection over a broad range of precipitation regimes within a single country. The northeastern Brazil is a semiarid region, with warm clouds and the organized convection influenced by the InterTropical Convergence Zone (ITCZ) and easterly waves. In the Amazon, the main targeted precipitation regimes are tropical Squall Lines (SL), local convection, which is strongly forced by the diurnal cycle and Mesoscale Convective Systems (MCS). In southern Brazil, there is the convection associated with cold fronts, Mesoscale Convective Complexes (MCC) and strongly electrified convection. This particular territorial extension also implies a surface type and land use heterogeneity, large coastline length and orography diversity. As the radiation in microwave has absorption and window channels that allow observing atmospheric constituents and cloud microphysics, the sensors in this spectrum have a greater ability to retrieve precipitation than visible and infrared sensors.

Satellite rainfall estimation (microwave, infrared, hybrid, etc.) has been widely used in Brazil for various purposes, e.g. for monitoring natural disasters, hydrological purposes and climatic applications. Although the quality of satellite rainfall estimate products has improved significantly in recent decades, such algorithms require careful validation studies, which aim to provide information about their quality, limitations and associated uncertainties.

Thus, the understanding and quantification of errors are extremely important for successful applications of satellite rainfall estimate products in hydrological modeling, data assimilation systems, climate studies and water management policy. Such analyses also contribute by providing insights to algorithm developers towards the improvement of precipitation estimation over a given location and surface type. In parallel, they are useful to verify algorithm efficiency in detecting precipitation type and monitoring precipitation system life cycles over certain regions.

Taking into account the absence of microwave precipitation retrievals adapted to reproduce such variability in Brazil, even more for operational purposes, and extensive validation of the H-SAF (EUMETSAT Satellite Application Facility on Support to Operational Hydrology and Water Management) PMW precipitation products over Brazil is of great importance towards the optimization of these products for this country. Currently the H-SAF products are optimized for Europe and Mediterranean area, and have been recently extended to Africa and Southern Atlantic.

In this context, the validation analysis, adaptation and application of the H-SAF products to Brazil will be of great importance as contribution to many sectors that would benefit from the operational use of satellite precipitation products such as weather monitoring/forecast, hydrological modeling, water and energy management, among others.

The objectives of this Visiting Scientist activity are:

1) Task 1 To select cases and to create the CHUVA ground-based radar dataset to be used for the validation.

2) Task 2: To generate the satellite precipitation datasets over the regions of interest for the selected cases.

3) Task 3 Adapt the H-SAF Common Validation Code provided by the H-SAF Validation Cluster to the selected datasets and verify the quality of the H-SAF precipitation products.

Before describing the methodology adopted for the single Tasks and discussing the results (Section 5, and 6), Section 2 is dedicated to briefly describe the CHUVA project while in Section 3 and Section 4 the ground-based radar configuration and the satellite precipitation products used in this work are presented.

## **2.THE CHUVA PROJECT**

The CHUVA Project was a research project aimed at the study of the cloud processes and precipitation through six field experiments held in Brazil during 2010-2014 (Table 1) in several regions characterized by different precipitation regimes, such as Alcântara-MA, Fortaleza-CE, Belém-PA, São José dos Campos-SP, Santa Maria-RS and Manaus-AM. The objective of the CHUVA field campaigns was to collect information about the cloud processes of the main precipitating systems over Brazil (e.g., squall lines in the Amazon; Mesoscale Convective Complexes [MCCs], cold fronts, middle latitude squall lines and the South Atlantic Convergence Zone [SACZ] in the southern region) in order to evaluate and improve quality of satellite-based precipitation estimates and knowledge of cloud microphysical processes (Machado et al., 2014). In addition, the observations from these regions provide a representative set of cases to evaluate the performance of the algorithms for different types of events.

The field campaigns in analysis on this study are highlighted in bold letters in Table 1.

Table 1 – Campaigns and periods of each CHUVA field experiments.

<b>Campaigns</b>	<b>Period</b>
<b>Fortaleza</b>	<b>3 – 29 April 2011</b>
Belém	1 – 30 June 2011
<b>Vale do Paraíba</b>	<b>1 Nov. 2011 – 3 March 2012</b>
Santa Maria	5 Nov. 2012 – 12 December 2012
<b>Manaus (IOP1)</b>	<b>13 Feb. – 31 March 2014</b>
Manaus (IOP2)	1 – 30 September 2014

### 3. GROUND-BASED REFERENCE: METEOR 50-DX

The validation of the H-SAF precipitation products over Brazil is carried out using as ground-based reference the precipitation rate estimates derived from the data collected by the mobile X-Band polarimetric radar during CHUVA Project.

The radar consists of a X Band dual-polarimetric radar manufactured by Gematronik (Germany) model METEOR 50-DX with the volume scan strategy including 13 elevations from 1.8° to 21.4°, and for all campaigns include a ZDR offset check and RHI scans.

The radar provides standard polarimetric parameters:

- reflectivity in horizontal polarization – ZH [dBZ];
- differential reflectivity – Z<sub>DR</sub> [dB];
- differential phase shift -  $\Psi_{DP}$  [deg];
- specific differential phase shift – K<sub>DP</sub> [deg /km];
- copolar correlation coefficient -  $\rho_{HV}$  [-];
- Doppler velocity – vD [m/s];
- velocity spectrum width -  $\sigma_{VD}$  [m/s].

To perform a correct validation procedure it is necessary to treat and minimize the large number of error sources associated with the radar system. Typically, the error sources can be associated to: radar calibration, ground clutter, rain attenuation, wet-radome attenuation, non-uniform beam filling, etc.

To be able to work with corrected data on the validation analysis, such treatment was developed by the Visiting Scientist HSAF\_CDOP2\_VS17\_01 (VS1) activity “Testing of dual polarization processing algorithms for radar rainfall estimation in tropical scenarios”. The data correction processing was made to eliminate or minimize the contamination of the most common error sources, and a quality indicator for each error source was identified. These quality indicators consisted of matrices of partial indexes, which compose an overall data quality index. The included indexes, are:

- 1) Ground clutter removal ( $q_{\text{clutter}}$ );
- 2) Partial Beam Blockage ( $q_{\text{PBB}}$ );
- 3) Range distance ( $q_{\text{range}}$ );
- 4) Non-uniform vertical profiles of reflectivity ( $q_{\text{VPR}}$ );
- 5) Differential phase processing ( $q_{\text{noise}}$ );
- 6) Attenuation correction ( $q_{\text{att}}$ ).

Besides the quality indexes procedure, another important aspect to be taken into account is the different parametrizations for the rainfall estimators. Traditionally, the simplest rainfall relation is the Z-R relation, where R is estimated from Z. With the availability of polarimetric variables it is possible to exploit their combinations (e.g., Z and  $Z_{\text{DR}}$ ) towards an optimal rainfall rate estimation. During VS1 several Z-R relations were analyzed. The results demonstrated that the relation showing best results compared to rain gauge data available during the campaign (Fortaleza, Vale do Paraiba and Manaus) is the one proposed by Vulpiani et al. (2015), hereafter indicated as Rq2Vu15 (please, refer to the VS1 intermediate report for details). For this reason, the X-band radar

precipitation rate estimates used for the H-SAF product validation are based on the Rq2Vu15 relation.

#### **4. SATELLITE PRODUCTS**

The passive microwave (PMW) precipitation products within the EUMETSAT H-SAF (Mugnai et al., 2013a) are based on the development and refinement of retrieval techniques exploiting all available radiometers in the GPM constellation, , and validation activity.

In this context, operational PMW precipitation products for the different radiometers are being released within H-SAF. They are based on two approaches (Mugnai et al., 2013b): the physically based Bayesian Cloud Dynamics and Radiation Database (CDRD) algorithm (Casella et al., 2013, Sanò et al., 2013) for conically scanning radiometers and the Passive microwave Neural network Precipitation Retrieval algorithm (PNPR) for cross-track scanning radiometers (Sanò et al., 2015, 2016). Three PMW H-SAF products have been considered within this VSA: H01 (CDRD approach applied to SSMIS), H02 (PNPR developed for AMSU/MHS), and H18 (PNPR adapted to ATMS). These products will be briefly described in the next sections with the purpose of reminding their main features useful to the interpretation of the results shown in this report.

##### **4.1 H01 – Cloud Dynamics Radiation Database (CDRD) for the conically scanning SSMIS radiometers**

The H01 is a precipitation retrieval algorithm based on the Bayesian physical approach for the conically scanning SSMIS radiometers onboard DMSP satellites (platforms F16, F17 and F18 are currently available). The SSMIS sensors are conical scanning radiometers equipped with 24 microwave channels ranging from 19GHz to 183GHz (most of the them in dual polarization), with 53.1° viewing angle and a swath of 1700km. The Bayesian approach requires *a priori* probability information which resides on a cloud-radiation database made up of thousands of micriphysical-meteorological profiles derived from cloud-resolving model simulations of different precipitation events including 60 simulations over the European/Mediterranean area (Casella et al., 2013) and 34

simulations over Africa and Southern Atlantic (Panegrossi et al, 2014). The algorithm has the database optimized for Europe, Africa and Southern Atlantic Ocean. Therefore, it does not include representative simulations from meteorological precipitating systems found in Brazil. H01 is operational and provides retrievals for the MSG full disk area. The nominal spatial resolution of the H01 corresponds to the IFOV of the SSMIS high frequency channels, which is around 15 km<sup>2</sup>. The product provides as final outputs: precipitation rate (mmh<sup>-1</sup>), the phase of the precipitation (solid, liquid, mixed, or unknown), and the quality index

#### **4.2 H02 - Passive Microwave Neural Network Precipitation Retrieval (PNPR) for AMSU and MHS cross-track radiometers**

The algorithm is based on a neural network approach and it operates for the cross-track scanning radiometers AMSU-A and MHS, currently flying on four satellites: NOAA-18, NOAA-19, MetOp-A and MetOp-B. Both radiometers were originally designed for temperature and water vapor sounding, respectively. The AMSU-A has 15 channels: 12 channels in 54 GHz oxygen band for temperature sounding and three additional window channels at 23.8GHz, 31.4 and 89GHz. MHS was designed for humidity sounding, with five channels: three channels in the 183GHz absorption line and two window channels at 89 and 150GHz. Both AMSU-A and MHS have a swath of about 2200km and a scan angle of  $\pm 48^\circ$  from nadir, while the AMSU-A takes 30 cross-track measurements and has a near-nadir spatial resolution of 48 km, the MHS (AMSU-B) takes 90 measurements and has a near-nadir spatial resolution of 16 km. Due to these characteristics, a variable sensor resolution (VSR) for H02 was defined according to the nominal resolution of AMSU-B/MHS, varying from 16km $\times$ 16 km/circular at nadir to 26km $\times$ 52 km/elliptical at scan edge. The training phase of the neural network is based on the same cloud-radiation database used for H01, optimized for Europe, Africa and Southern Atlantic Ocean. Therefore, The product provides as final outputs: precipitation rate (mmh<sup>-1</sup>), the phase of the precipitation (solid, liquid, mixed, or unknown), and the quality index

### **4.3 H18 - Passive Microwave Neural Network Precipitation Retrieval (PNPR) for ATMS cross-track radiometer**

The product H18 for ATMS is based on the evolution of the PNPR algorithm with respect to the previous version (H02) developed for AMSU/MHS radiometers, adapted to better exploit of the capabilities of the new sensor. The ATMS radiometer is a cross-track scanning microwave radiometer currently on board of the Suomi NPP satellite with a swath of 2600 km and angular span of  $\pm 52.77^\circ$  relative to nadir, and with 22 channels, ranging from 23 to 183 GHz, providing both temperature and humidity soundings. The radiometer has three new channels compared to AMSU/MHS: channel 4 (51.76GHz) for the lower tropospheric temperature sounding and the channels 19 and 21 (183.31 $\pm$ 4.5 and 183.31 $\pm$ 1.8GHz) to improve the moisture profiling. The beamwidth changes with frequency and is  $5.2^\circ$  for channels 1–2 (23.8–31.4 GHz),  $2.2^\circ$  for channels 3–16 (50.3–57.29 and 88.2 GHz), and  $1.1^\circ$  for channels 17–22 (165.5–183.3 GHz) with corresponding nadir resolutions being: 74.78, 31.64, and 15.82 km, respectively.

Relative to the algorithm design the H18, differently from H02, has a unique NN capable of operating on the whole MSG disk area regardless of the type of surface. The two new channels 19 and 21 (183.31 $\pm$ 4.5 and 183.31 $\pm$ 1.8GHz) are exploited, and the canonical correlation analysis is used to find the linear combinations of TBs best correlated with surface precipitation rate. The product provides as final outputs: precipitation rate ( $\text{mmh}^{-1}$ ), the phase of the precipitation (solid, liquid, mixed, or unknown), and the quality index and provides the output on a grid corresponding to the ATMS nominal resolution of the high-frequency channels, varying from  $15.82 \text{ km} \times 15.82 \text{ km}$ /circular at nadir to  $68.4 \text{ km} \times 30.0 \text{ km}$ /elliptical at scan edge. The training of H18 was performed using the same cloud radiation database used for H01 and H02, representative of the MSG full disk area.

## **5. Methodology**

### **5.1 TASK 1: Selection and preparation of CHUVA Dataset**

The first part of this work consists on the verification and selection of the useful information from the CHUVA dataset from each campaign to be used for the validation of the satellite precipitation products. It was necessary to analyze all the CHUVA campaign radar data to be able to start developing a robust and efficient quantitative precipitation estimation (QPE) processing chain able to identify the most common error sources. Considering the dataset available, the proposed methodology was verified for and applied to the Fortaleza, Manaus and Vale do Paraíba campaigns. Furthermore, the radiosondes data and pluviometric data were provided.

#### **5.1.1 Fortaleza Campaign**

The focus of the campaign in Fortaleza was to analyze warm-cloud processes and deep convection associated with the intertropical convergence zone (ITCZ). Therefore, a volume scan strategy was implemented with 13 elevations focusing on both the lower and upper troposphere (i.e., warm and deep cloud types). As already mentioned, the strategy for all campaigns included a  $Z_{DR}$  offset check, and Range Height Indicator (RHIs) scans. For Fortaleza, two RHI scans were performed: one over the main site and another at  $180^\circ$ , perpendicular to the coast, where most systems propagate into the continent. Three complete scans (volume scan, RHIs, and vertically pointing) were run in 20-min cycles and a zero check (background noise estimation) was performed once per hour.

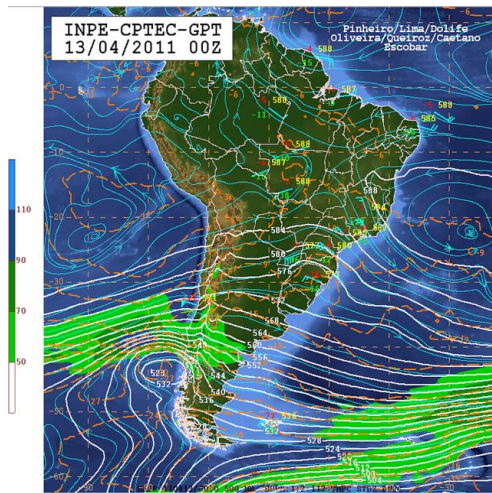
The maximum rainfall intensity recorded during the campaign was  $152 \text{ mm h}^{-1}$ , with the drop size distributions (DSDs) revealing a large population of large ( $>4 \text{ mm}$ ) raindrops. Fortaleza had the largest average vertically integrated water vapor ( $56.1 \text{ mm}$ ) and the highest melting level ( $4.7 \text{ km}$ ). These characteristics suggest that the rainfall events in Fortaleza appear to have a very important warm process when producing rain drops. Additionally, the stratiform rainfall in Fortaleza exhibited the highest and least prominent brightband (BB) peak intensity (Calheiros and Machado, 2014).

The six precipitating events selected (Table 2) for the validation analysis comprise basically similar synoptic configuration and precipitation pattern. The weather conditions on these days, with the exception for 24th April, was the presence of the Intertropical Convergence Zone (ITCZ) in its Southern position, acting over the northeast region of Brasil. Associated with it, the wind flow was transporting humidity from the ocean to the coast, helping to enhance and trigger the convective processes.

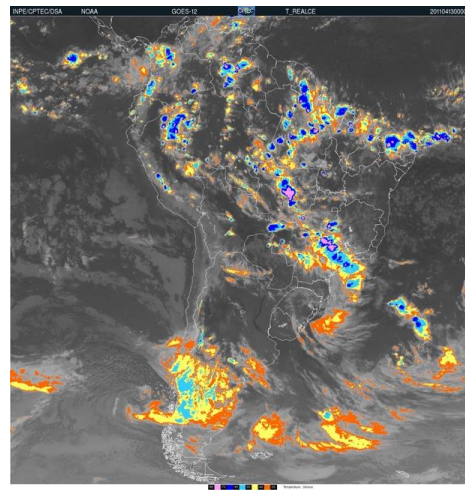
Table 2 – Precipitating events selected from Fortaleza Campaign.

Dates	Precipitating systems
13/04/2011	ITCZ (stratiform precipitation and bright band)
15/04/2011	ITCZ (convective and stratiform system)
24/04/2011	VCAN (High Level Cyclonic Vortice)
25/04/2011	ITCZ (stratiform precipitation and bright band)
26/04/2011	ITCZ (convective cells and stratiform precipitation and bright band)
29/04/2011	ITCZ (stratiform precipitation)

Figure 1 exhibits the synoptical configuration from 13th April (which does not differ from the other cases) where it is possible to see the confluence of wind on the northeastern coast until in 500hPa level (Fig. 1a), and the instability associated with the ITCZ can be seen on the enhanced satellite image from 13/04/2011 at 00:00UTC over the northeast region of the country represented by the low IR brightness temperature shown in Fig. 1b. The next figures (Fig. 2 and 3) show the RHI of two rainfall events (13/04/2011 and 25/04/2011) where it is possible to verify the vertical structure of the precipitating systems with typically stratiform features, and a bright band around 5 km of altitude, and, in some cases, the presence of isolated convective cells.



a)



b)

Figure 1 – a) Technical bulletin of synoptical conditions on 13<sup>th</sup> April, 2011 at 00:00UTC at surface (left) and b) Infrared enhanced on 13<sup>th</sup> April, at 00:00UTC.

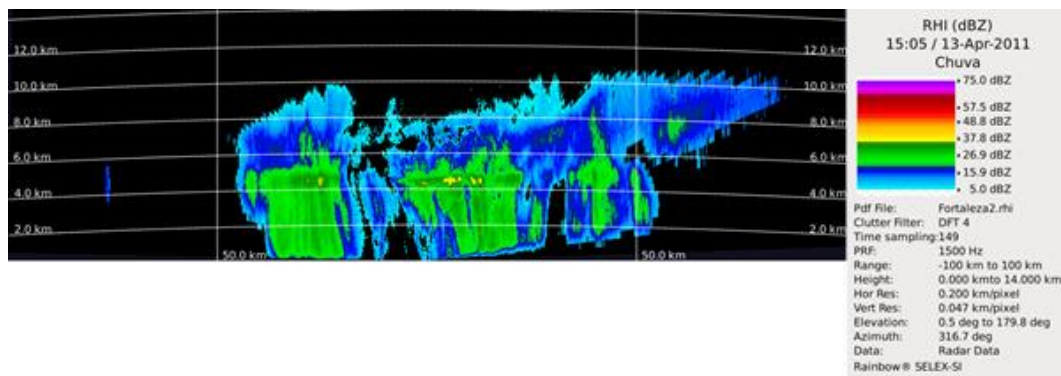
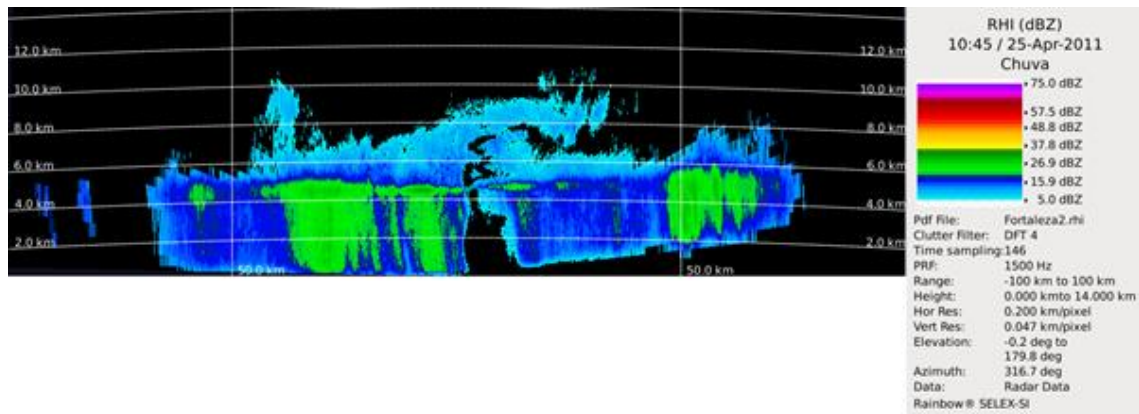


Figure 2 - RHI (Range Height Indicator) of a meteorological system observed over Fortaleza on 13/04/2011 at 15:05 UTC.

a)



b)

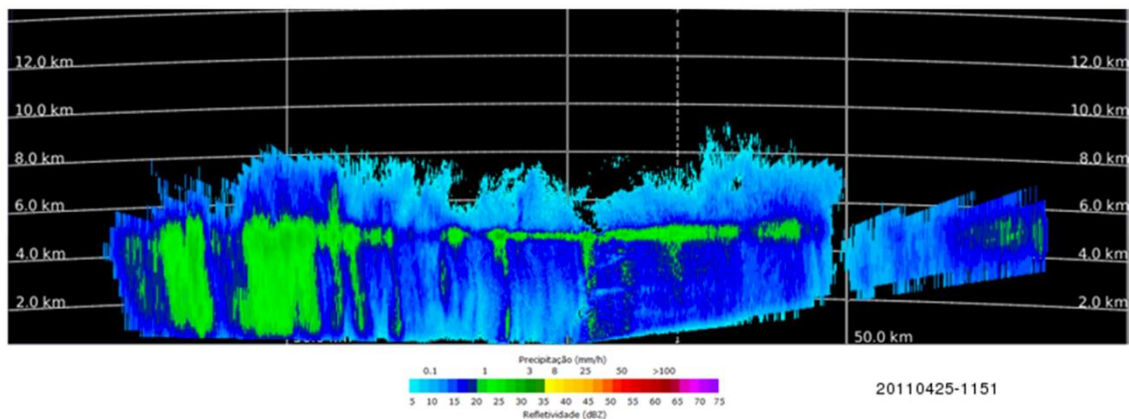


Figure 3 - RHI (Range Height Indicator) of a meteorological system observed over Fortaleza on 25/04/2011 at a) 10:45UTC and b) 11:51UTC.

### 5.1.2 Vale do Paraíba Campaign

The Vale do Paraíba campaign had the longest duration, with an IOP from 1 November to 22 December 2011, followed by a second period with less intensive measurements through 31 March 2012. The instrumentation was installed along a line perpendicular to the coast. The radar was 90 km inland from the ocean at an elevation of 650 m. The main site was installed 11 km from the radar, and a succession of sites (spaced by approximately 20 km) was installed along a line perpendicular to the ocean. The radar strategy was designed to run for 6 min.

The primary objective of this campaign was to study storm electrification. During the Vale do Paraíba campaign, several intense thunderstorms

and some severe weather events were recorded, including a downburst, causing destruction of many trees, and many cases of hailstorms. The rain rate at the 99th percentile at the main site was 137 mm h<sup>-1</sup>. Warm clouds during the Vale do Paraíba campaign had a lower frequency and average rain rate than the other CHUVA tropical sites. From this campaign, the selected cases to be analysed on the validation are described in Table 3.

Table 3 – Precipitating events selected from Vale do Paraíba Campaign.

Dates	Precipitating systems
11/11/2011	Local Convection
13/11/2011	Stationary frontal system
01/12/2011	ZCAS (South Atlantic Convergence Zone)
08/12/2011	Local Convection
14/12/2011	Severe Convection
20/12/2011	ZCAS (South Atlantic Convergence Zone)

Differently from the other campaigns, the events from Vale do Paraíba are clearly of intense convective nature, as verified through the following examples.

On 13/11/2011 at 23:12 UTC the reflectivity at 2km (CAPPI) revealed the significantly convective activity on the eastern region of São Paulo State with the highest values around 50dBz (Fig. 4a). Even though the precipitation was detected starting at 20 UTC, the electrical activity started before, with recording of pulses in VHF from the 17 UTC with a maximum density of more than 1.000 pulses per 4 km<sup>2</sup>. The daily density of the VHF pulses detected by the LMA network is show in Fig. 4b.

a)



b)

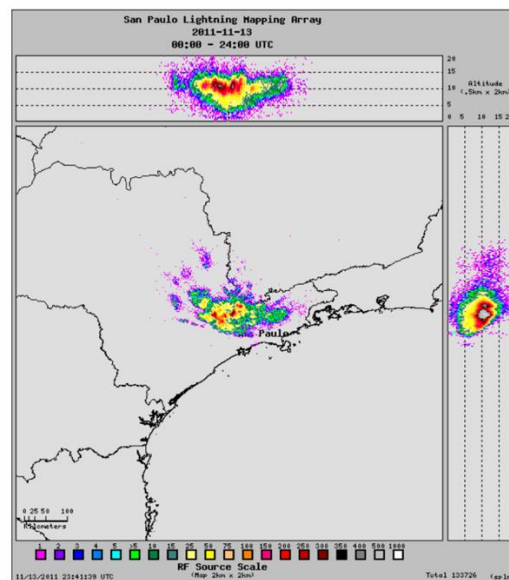
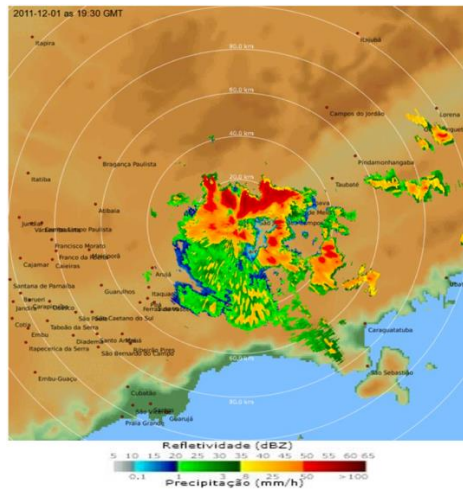


Figure 4 – a) CAPPI of 2 km of X-Band Radar at 23:12 UTC on 13/11/2011 localized on UNIVAP site (São José dos Campos city) and b) daily density of electromagnetic pulses in VHF of the LMA network with resolution of 2 km x 2 km.

In Fig. 5 the CAPPI at 2km of the X-Band Radar shows the occurrence of intense convective cells in the vicinity of São José dos Campos city on 01/12/2011 at 19:30UTC. The reflectivity reached values around 60 dBz. During the early evening high electrical activity was also observed (Fig. 5b) in the east of São Paulo city and Vale do Paraíba region reaching a maximum of 200 sources/4 km<sup>2</sup> /day at approximately 10 km in height. The hourly analysis of the LMA

information also showed that the maximum occurrence of electric activity near São José dos Campos was between 19-20 UTC with approximately 12.5 sources/km<sup>2</sup>/hour.

a)



b)

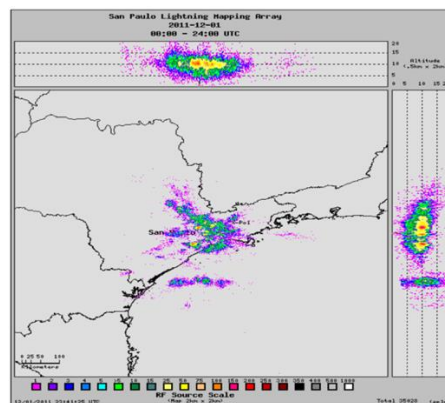


Figure 5 – a) CAPPI of 2 km of X Band Radar at 19:30 UTC on 1/12/2011 localized on UNIVAP site (São José dos Campos city) and b) density of electromagnetic pulses in VHF daily of the LMA network with resolution of 2 km x 2 km.

### 5.1.3 Manaus Campaign

Table 4 shows the precipitating events selected from Manaus campaign.

Table 4 – Precipitating events selected from Manaus Campaigns.

Dates	Precipitating systems
15/02/2014	Convective and stratiform rain
21/02/2014	Squall lines
23/02/2014	Squall lines with large stratiform extension
24/02/2014	Squall lines
25/02/2014	Sparse convective cells
26/02/2014	Convective and stratiform rain
02/03/2014	Convective and stratiform rain (during the night)
08/03/2014	Stratiform systems with large extension
28/03/2014	Stratiform system

Figure 6 shows the evolution of well-defined squall line with defined convective and stratiform portions. At 08:50 UTC (Fig. 6b), the line approached Manacapuru (radar location), presenting maximum reflectivity greater than 50 dBZ and it is also possible to observe the gust front as a curved line of smaller reflectivity closer to Manacapuru. At 09:10 UTC (Fig. 6c), the convective line reached Manacapuru. After the initial convective rain, the stratiform portion of the line approached Manacapuru and lasted until about 13:40 UTC (Fig.6d).

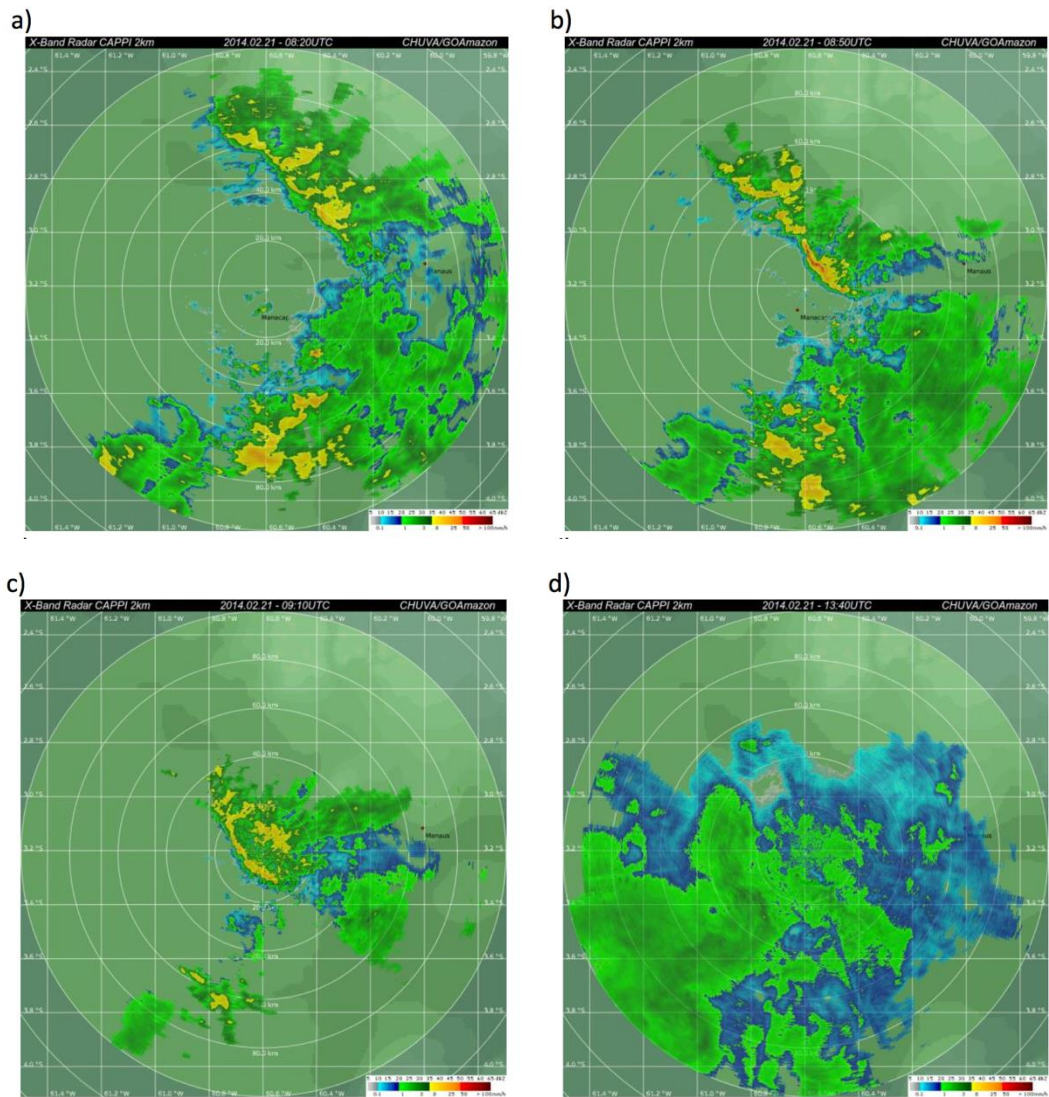


Figure 6 - Radar X-Band (CAPPI of 2km) of the events which acted on February, 21, a) 08:20 UTC, b) 08:50 UTC, c) 09:10 UTC, d) 13:40 UTC.

Another example of a precipitation system occurred in Manaus is presented in Fig. 7 characterized by several sparse convective cells, that persisted all day. The convective rain over Manacapuru (radar location) was observed at 18:46 UTC, with reflectivity values higher than 50dBZ, relative to about 50 mm/h rainfall, and presented cloud tops around 14 or 15 km (Fig. 7d).

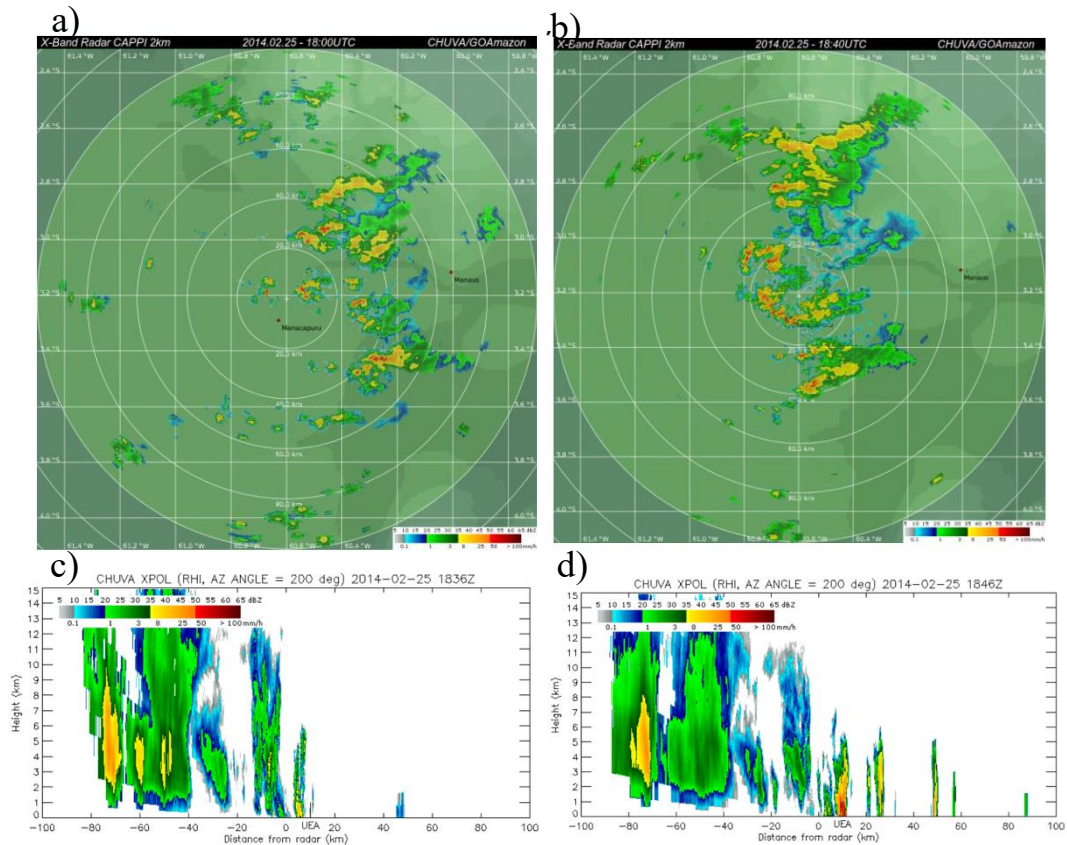


Figure 7 - Radar X-Band (CAPPI of 2km) of the events which acted on February, 25, a) 18:00 UTC, b) 18:40 UTC and RHI at c) 18:36 UTC, d) 18:46 UTC.

For each selected case, the ground-based radar estimates provided by the VS1 have been analyzed, and processed as described in Section 7.

## 5.2 TASK 2: Satellite dataset generation

To be able to perform the validation, it was necessary to proceed with the verification and acquisition of the satellite overpasses for the period of the CHUVA experiments, and to reprocess the H-SAF products for the period and regions selected to create the dataset to be validated.

All the orbit files containing the brightness temperatures (TBs) to be used as input data for each rainfall retrieval algorithm to generate the precipitation rate estimates (H01, H02, and H18) were downloaded from the NOAA website (<https://www.class.ngdc.noaa.gov/saa/products/>). The procedure used for each product is described in Table 5. It was necessary to enlarge to the West (extended to 75°N-60°S and 80°W-80°E) the area for which each algorithm was

designed to include the entire Brazil, and for each product all the data available for the period of the CHUVA campaign were processed. Finally, it was necessary to convert H01, H02 retrieval output in BUFR format, to be able to use the common validation code. While for the Manaus campaign the three products, H01, H02 and H18 were analyzed, for the other two campaigns, Fortaleza and Vale do Paraiba, only H01 and H02 were considered because the ATMS was not available in 2011.

Table 5 - Satellite sensors features and technical informations relative of each algorithm.

<b>SSMIS (H01)</b>	
Source	NOAA Web Site (select overpasses from NOAA Web Site)
Satellites	DMSP Satellites
Format	Binary Files, NetCDF Format (ECMWF data)
File type	Complete orbit
Problems	Understand which satellites can be used (there are malfunctions)
<b>AMSU-A, AMSU-B and MHS (H02)</b>	
Source	NOAA Web Site
Satellites	NOAA-18, NOAA-19 , MetOp-1 and MetOp-B
Format	Binary files, 1B (Use of AAPP to convert in 1C*)
File type	Complete orbit
Problems	Erros in scan lines
<b>ATMS (H18)</b>	
Source	NOAA Web Site
Satellites	Suomi-NPP
Format	HDF5
File type	Fragmented orbit
Problems	Check the correct combining of the fragments to remove any repetition of the scanning lines

### 5.3 TASK 3: Application of the Common Validation Code

The common validation code (CVC) developed by the Precipitation Product Validation Group (PPVG) [Puca et. Al, 2014] enables to implement a common validation procedure to be adopted by each institution in the H-SAF Validation cluster to make the validation results comparable. The common validation methodology for the treatment of the ground-based radar (and raingauge) data produces statistical scores (multi-categorical and continuous) and case study analysis (Rinollo et al., 2013). The products to be validated differentiate in terms of retrieval technique, spatial and temporal resolutions.

Therefore, each product requires a specific validation procedure configured to its characteristics. The methodology can be divided on the follow general steps:

- Ground data error analysis;
- Upscaling of radar data to match the satellite product nominal resolution;
- Temporal matching of precipitation products (satellite and ground).
- Application of evaluation statistical methods (continuous and multi-categorical) to all available overpasses, for each pixel pair (satellite-ground).

To be able to use the CVC on the the Brazilian radar data it was necessary to adapt the code by including the new radar coordinates (Fortaleza, Manaus and Vale do Paraíba) and by reading the new radar data. It was also necessary to adapt the code to read the NetCDF format for the H18 (PNPR-ATMS) product (differently from H01 and H02 which generate the ouput in BUFR format).

The CVC was configured with a maximum time difference to find the temporal matching between satellite and radar data of 16 minutes . The radar data was up-scaled to the satellite product nominal resolution, considering the antenna pattern (Gaussian function), viewing geometry, and scanning strategy (conical and cross-track) of the MW radiometer. As the radar data was filtered before (quality control), the pixels with low quality are eliminated of the upscale processing.

To investigate the performance of the precipitation products, the statistical scores commonly used in the pixel-based validation by H-SAF PPVG were considered. Table 6 presents the scores formulation for continuous statistical scores and Table 7 for multicategory scores. Additionally, with intent to identify a reasonable quality control for each data campaign, the scores were generated for quality control larger than 0,5, 0,6 and 0,7.

Table 6 – List of continuous statistical scores.

Score	Acronym	Range	Perfect Score	Calculation
Mean Error or Bias	ME	$-\infty$ to $+\infty$	0	$ME = \frac{1}{N} \sum_{k=1}^N (sat_k - obs_k)$
Standard Deviation	SD	0 to $+\infty$	0	$SD = \sqrt{\frac{1}{N} \sum_{k=1}^N (sat_k - obs_k - ME)^2}$
Root Mean Square Error	RMSE	$\geq 0$	0	$RMSE = \sqrt{\frac{1}{N} \sum_{k=1}^N (sat_k - obs_k)^2}$
Fractional Standard Error	FSE	$\geq 0$	0	$FSE = \frac{\sqrt{\frac{1}{N} \sum_{k=1}^N (sat_k - obs_k)^2}}{\frac{1}{N} \sum_{k=1}^N obs_k} = \frac{RMSE}{\frac{1}{N} \sum_{k=1}^N obs_k}$
Correlation Coefficient	CC	-1 to 1	1	$Correlation\ coefficient - r = \frac{\sum (F - \bar{F})(O - \bar{O})}{\sqrt{\sum (F - \bar{F})^2} \sqrt{\sum (O - \bar{O})^2}}$

Table 7 - Multicategory statistical scores.

Probability Of Detection	POD	0 to 1	1	$POD = \frac{hits}{hits + misses} = \frac{hits}{observed\ yes}$
False Alarm Rate	FAR	0 to 1	0	$FAR = \frac{false\ alarms}{hits + false\ alarms} = \frac{false\ alarms}{forecast\ yes}$
Critical Success Index	CSI	0 to 1	1	$CSI = \frac{hits}{hits + misses + false\ alarm}$

## 6. RESULTS

### 6.1 Statistical evaluation

With the application of the CVC, it is possible to analyse all the matched pixel pairs between the radar data and satellite overpass. The continuous statistical scores were computed for the pixels in which both radar and satellite give rainfall estimation larger than zero (hits only), otherwise the scores may result in smoothed values by the large amount of zero filled pixels. Thus, henceforward the considered values shown in the tables are relative to the hits. For the multicategory scores all pixels are considered (including zero filled pixels).

The first analysis was made for Fortaleza campaign, but unfortunately it was verified that despite de application of a extensive quality control y the VS it as noticed that data still contained some significative errors, probably associated

with some non treated issuea on the raw data. For this reason, the analysis made on the Fortaleza data will not be shown on the follow analysis.

For Manaus, the events under analysis had a total number of 33 overpass matchings (which means correspondence in time and space of both the satellite and radar measurements) for H01, 49 matchings for H02 and 13 matchings for H18. Analyzing the behavior of the scores for H01 (Table 8 and Table 9) it is evident that as the quality index present an improvement on the scores, (i.e., RMSE goes from 7,19 to 5,20 and SD from 5,16 to 3,69). It is important take into account that the pixel sample becomes smaller and smaller and it is difficult to extrapolate and say that this a generic trend of improvement for H01. The multicategory scores present a relatively good values of POD (around 0,77), but also a high FAR values (around 0,60) which means that H01 is detecting precipitation where the radar does not see precipitation.

Table 8 – Continuous statistical scores for H01 for Manaus, with 905, 672 and 406 pixels for the respective threshold of quality index (QI) (0.5, 0.6, 0.7)..

PRODUCT H01	Sat. mean	Rad. mean	ME	RMSE	SD	FSE	CORR
QI > 0,5	6,10	1,10	5,00	7,19	5,16	6,49	0,35
QI > 0,6	5,34	0,98	4,35	5,93	4,03	6,00	0,46
QI > 0,7	4,60	0,93	3,67	5,20	3,69	5,59	0,40

Table 9 – Multicategory statistical scores for H01 for Manaus with 7090, 5108 and 3149 pixels for the respective threshold of quality index (QI) (0.5, 0.6, 0.7)..

PRODUCT	POD	FAR	CSI
H01			
QI > 0,5	0,77	0,60	0,35
QI > 0,6	0,77	0,57	0,38
QI > 0,7	0,75	0,54	0,39

Table 10 and 11 show the scores for H02 for Manaus. It is worth noting that H02 has in general slightly better scores than for H01, such as lower mean rainfall rate values, ME, RMSE, SD and FSE. In Table 11 the POD has good values (0,96) and the FAR is slightly lower than H01 (around 0,52). Despite the larger number of pixels, H02 does not show a trend with increasing quality index (Table 10). This can be due the resolution of H02 that is lower with respect to H01 and, consequently, the scores are evaluated on the basis of a larger number of radar data per satellite pixel compared to H01. Therefore, the quality index was not selective enough to impact positively the scores. For H02 it would be worth testing higher quality index but the sample size would be too small in this case, and not statistically significant.

Table 10 – Continuous statistical scores for H02 for Manaus with 1085, 907 and 631 pixels for the respective threshold of quality index (QI) (0.5, 0.6, 0.7).

PRODUCT H02	Sat. mean	Rad. mean	ME	RMSE	SD	FSE	CORR
QI > 0,5	4,20	1,14	3,06	5,48	4,54	4,79	0,31
QI > 0,6	4,08	1,13	2,95	5,40	4,53	4,75	0,30
QI > 0,7	3,78	1,18	2,59	5,11	4,40	4,32	0,32

Table 11 – Multicategory statistical scores for H02 for Manaus with 3757, 2986 and 1889 pixels for the respective threshold of quality index (QI) (0.5, 0.6, 0.7)..

PRODUCT H02	POD	FAR	CSI
QI > 0,5	0,96	0,54	0,44
QI > 0,6	0,96	0,52	0,46
QI > 0,7	0,96	0,47	0,51

Since ATMS is onboard just one satellite, the number of overpasses over the region of interest is lower than the other sensors. Consequently, the number of pixels is too low to establish the ideal quality index for the region (Tables 12 and 13). As for H02, for quality index does not have an impact on the scores if it is lower than 0.6. For H18, it is necessary to use a larger sample of reference data. Similarly to H02, the H18 has better statistical scores than H01, with lower mean values, ME, RMSE, SD and FSE in comparison to H01. The muticategory scores shows intermediate values (POD around 0,86 and FAR around 0,45) in comparison to H01 and H02.

Table 12 – Continuous statistical scores for H18 for Manaus with 227, 198 and 140 pixels for the respective threshold of quality index (QI) (0.5, 0.6, 0.7)..

PRODUCT H18	Sat. mean	Rad. mean	ME	RMSE	SD	FSE	CORR
QI > 0,5	4,01	1,11	2,90	4,63	3,61	4,16	0,36
QI > 0,6	4,00	1,19	2,80	4,65	3,71	3,87	0,36
QI > 0,7	4,53	1,46	3,07	5,10	4,07	3,48	0,34

Table 13 – Multicategory statistical scores for H18 for Manaus with 3757, 2986 and 1889 pixels for the respective threshold of quality index (QI) (0.5, 0.6, 0.7).

PRODUCT H18	POD	FAR	CSI
QI > 0,5	0,83	0,49	0,45
QI > 0,6	0,83	0,45	0,48
QI > 0,7	0,81	0,39	0,53

For the cases of Vale do Paraiba campaign corresponded to 27 overpass matchings (satellite x radar) for H01 and 31 matchings for H02 (H18 is not considered because ATMS was not available in 2011-2012). The respective statistical scores are presented in Tables 14, 15, 16 and 17. For both products H01 and H02, the statistical scores do not show a significant trend with the quality index, because the sample size is small and the number of pixels gets lower as the quality index threshold increases. Anyway, the threshold of 0,5 filters the sample (compare to the case when no quality control is used, not shown) eliminating the pixels associated with the most prevalent error sources. The ME is very small (for

example compared to the scores in Manaus), close to zero or slightly negative. This shows that either that the H01 has a better performance in this region, or that the radar rainfall estimation is more reliable over this region. The POD has lower values than for Manaus (from 0, 34 to 0,62), but the FAR is slightly lower. The small sample size, however, does not allow to completely rely on these results, suggesting that a case study analysis might be very useful in this region.

Table 14 – Continuous statistical scores for H01 for Vale do Paraiba with 368, 287 and 181 pixels for the respective threshold of quality index (QI) (0.5, 0.6, 0.7)

PRODUCT H01	Sat. mean	Rad. mean	ME	RMSE	SD	FSE	CORR
QI > 0,5	2,74	2,81	-0,07	3,78	3,77	1,34	0,39
QI > 0,6	2,67	2,88	-0,2	3,83	3,82	1,32	0,44
QI > 0,7	2,53	2,89	-0,35	4,00	3,98	1,38	0,44

Table 15– Multicategory statistical scores for H01 for Vale do Paraiba with 3569, 3197 and 2420 pixels for the respective threshold of quality index (QI) (0.5, 0.6, 0.7).

PRODUCT H01	POD	FAR	CSI
QI > 0,5	0,62	0,42	0,42
QI > 0,6	0,57	0,45	0,38
QI > 0,7	0,49	0,49	0,33

Table 16 – Continuous statistical scores for H02 for Vale do Paraíba with 187, 175 and 124 pixels for the respective threshold of quality index (QI) (0.5, 0.6, 0.7).

PRODUCT H02	Sat. mean	Rad mean	ME	RMSE	SD	FSE	CORR
QI > 0,5	2,61	2,35	0,25	3,55	3,54	1,50	0,30
QI > 0,6	2,54	2,35	0,18	3,57	3,57	1,51	0,27
QI > 0,7	2,45	2,76	-0,30	3,56	3,55	1,29	0,37

Table 17 – Multicategory statistical scores for H02 for Vale do Paraíba with 1445, 1320 and 991 pixels for the respective threshold of quality index (QI) (0.5, 0.6, 0.7)

PRODUCT H02	POD	FAR	CSI
QI > 0,5	0,50	0,23	0,43
QI > 0,6	0,49	0,22	0,42
QI > 0,7	0,43	0,21	0,39

## 6.2 Pixel by pixel analysis

To add additional information about the product performances, a case study analysis, with example of the pixel by pixel comparison, is carried out and presented bellow.

Figure 8a,b present a case study for Manaus, on 21/12/2014. Figure 8a shows the overall quality index associated to the radar rainfall filed at its original resolution, showed in Fig. 8b. On this day, a well defined squall line approached the X-Band radar region. The systems insisted on the region from the morning around 08:20UTC until the afternoon 15:40UTC. It is possible to see the presence of convective cores with rainfall rate up to 35 mm/h in the regions between the North-West to South-West quadrants. The remaining regions are dominated by light and stratiform precipitation with rainfall rates up to 6 mm/h.

The precipitation field upscaled to the satellite native grid, the respective H01 estimation, and associated quality index map are shown in Fig. 9. The results are shown for: a)  $QI > 0,5$ , b)  $QI > 0,6$  and c)  $QI > 0,7$ .

It is noted that H01 tends to detect precipitation over areas where the radar doesn't detected precipitation (gray pixels Fig. 9a), which is related to the high values of FAR (around 0,60) found for Manaus. The light rain rate provided by the radar (dark blue), is associated to moderate precipitation values by H01 (light blue). Similarly, to the higher estimates by the radar (light blue) correspond higher rain rates by H01, ranging from 10 to 30 mm/h (light blue to red). Comparing the maps a, b and c, it can be noticed that the increase of the quality index impacts positively the scores, eliminating the spurious pixels (usually more distant from the center of the radar) that, in this case, correspond to the satellite pixels associated to the larger overestimation. In this case, it is expected an improvement in the statistics with the increase of the quality control as seen on the Table 8 and Table 9.

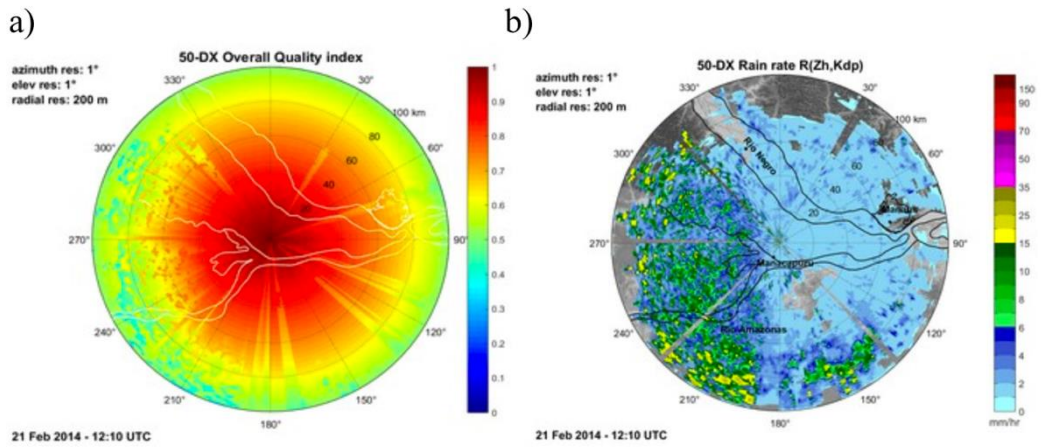


Figure 8 - a) Overall quality index radar and b) Rain rate from radar on 21/02/2014 at 12:10UTC.

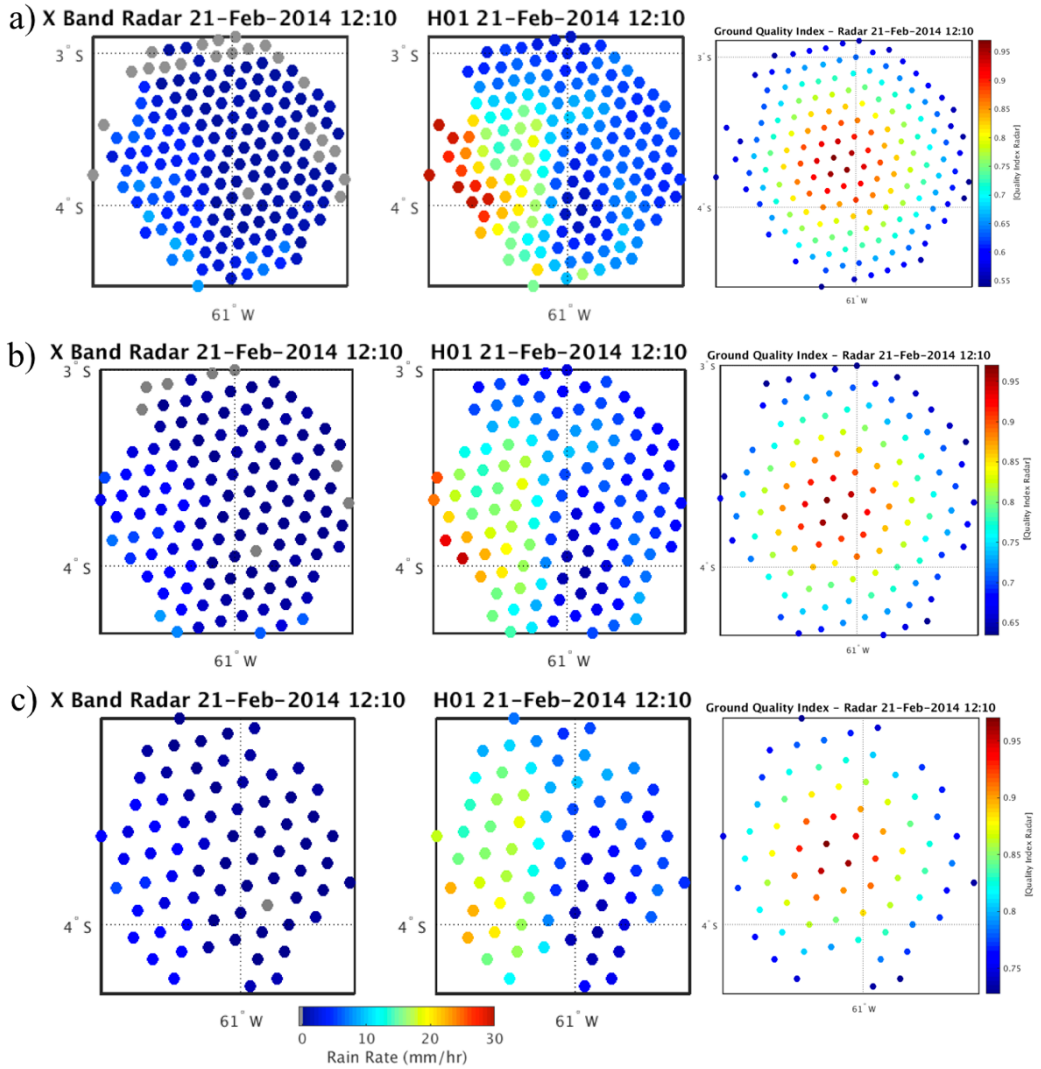


Figure 9 – Rain rate from radar upscaled to the satellite grid (left), H01 rain rate (center) and overall quality index map (right) in Manaus on 21/02/2014 at 12:10

for a) quality index  $> 0,5$ , b) quality index  $> 0,6$  and c) quality index  $> 0,7$ .

For H02, the case on 08/03/2014 at 05:30UTC is shown in Fig. 10 and 11. It is possible to see the presence of convective cells on the border of the Rio Negro and also some small convective cells over the southeastern quadrant (Fig. 10b).

It is evident that also H02 detects precipitation over a larger area than the radar (gray pixels Fig. 11a), as shown by the high values of FAR (around 0,50) in Table 11. It is worth noting that the detection of the precipitation is related to the screening procedure, which is the part of the algorithm where potential precipitating pixels are identified.

An interesting aspect to highlight is that in correspondence of the most intense precipitation estimated by the radar (Fig. 10b), the upscaled map show only one radar pixel (around 12 mm/h), whereas the H02 show more pixels with high precipitation (20-25 mm/h). With the increase of the quality index threshold it is possible to see the reduction of spurious pixels, as evidenced by the slightly improvement FAR values in Table 11.

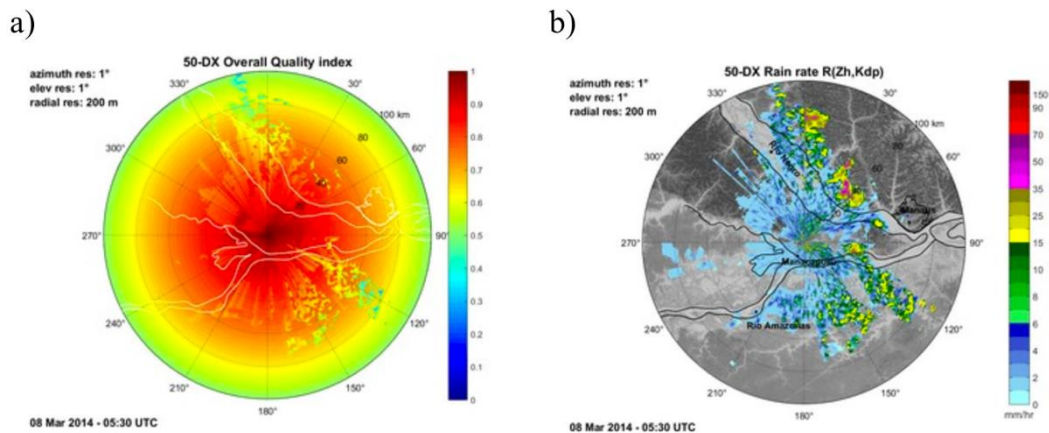


Figure 10 - a) Overall quality index radar on and b) Rain rate from radar on 08/03/2014 at 05:30UTC.

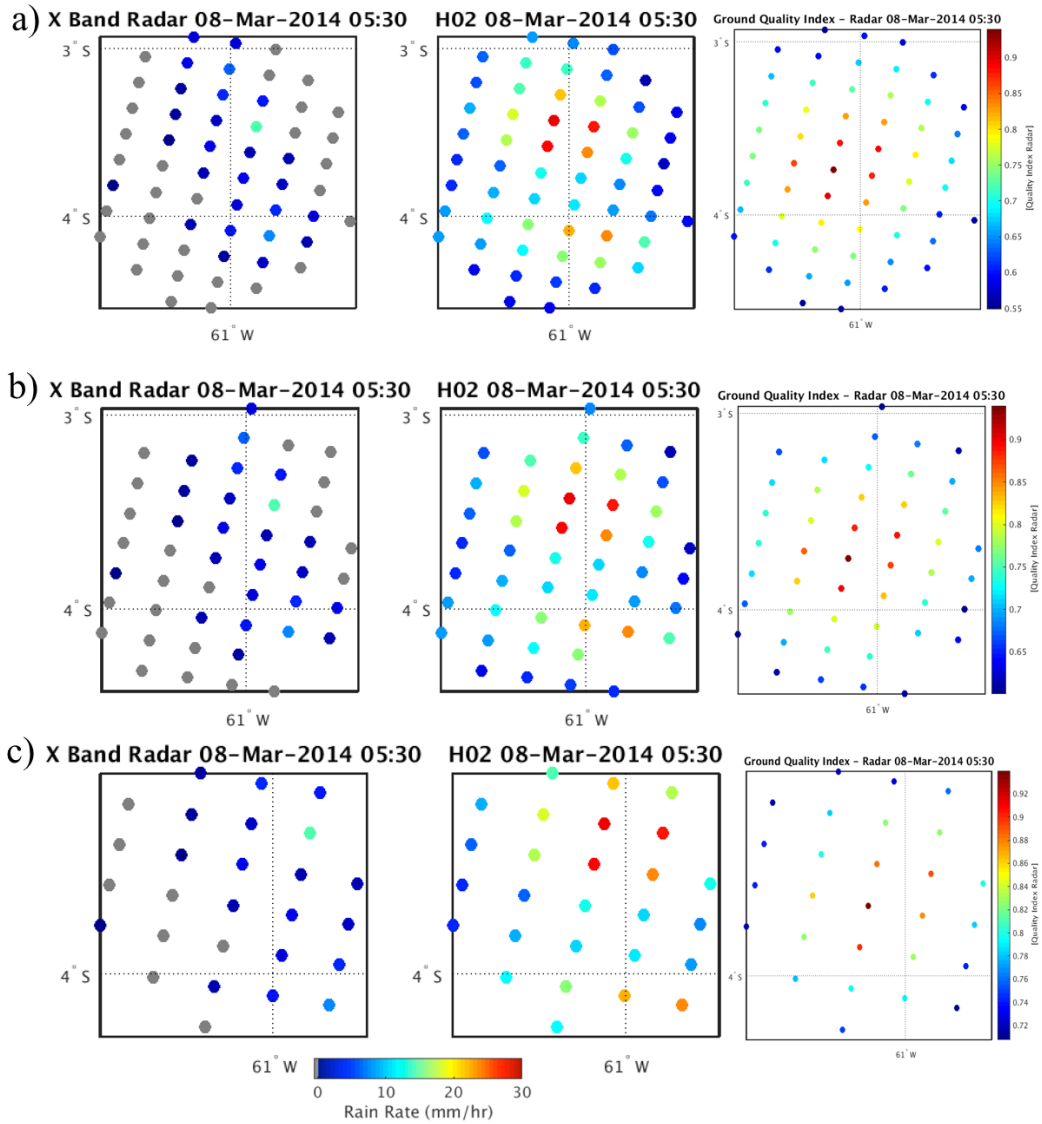


Figure 11 – Rain rate from radar upscaled to the satellite grid (left), H02 rain rate (center) and overall quality index map (right) in Manaus on 08/03/2014 at 05:30UTC for a) quality index > 0,5, b) quality index > 0,6 and c) quality index > 0,7.

The case study for H18 refers to the same event presented for H02, on 08/03/2014 but at 05:10 UTC. Since the ATMS overpass is close of the AMSU/MHS overpass examined in Fig. 11 (20 minutes before), the radar pattern is similar. However, we can see slight differences in H18 compared to H02, even though the spatial pattern shows the same behavior as H02 because both products are based on the same precipitation screening method.

It is worth pointing out that the screening of precipitation is equal for all products used in this analysis. Basically, the precipitation screening is based on

three channels, being:  $TB_{183+3}$  and  $tb_{183+7}$  which are water vapor absorption band at 183.3 GHz and the  $TB_{53.6}$  in the oxygen absorption band around 50 GHz. Manaus is within the Amazon forest and is characterized by high water vapor content, and in this conditions the weighting functions of the 183.3 GHz channels peak at high levels. This can, affect the efficiency of the screening in the identification of potential precipitating pixels, especially when the clouds are not very deep, as they appear to be during the wet season in the Amazon region. Another important feature is the surface characterization in the algorithms, which does not represent the complexity due the presence of two rivers in contrast to the forest and to the urban area of Manaus. This scenario is flagged in the algorithm as coastal region, usually associated to larger uncertainties in PMW retrieval algorithms.

On the other hand, the H18 tends to produce a lower overestimation compared to H02. This aspect is related to the retrieval algorithm itself, which is quite different for H02 and H18 . The essential change is that H18 is based in just one neural network for all surface types, and it is trained with a unique training database. Two new ATMS channels in the water vapor absorption band (at  $183.31\pm 4.5$  and  $183.31\pm 1.8$  GHz) are considered in the input to the neural network. The contribution of the new channels (i.e., the TB difference) provides additional information on the clouds that is not available when using the other channels at 183.3 GHz (for example for MHS). The number of pixels is reduced by the quality control application, but in this case the impact on the statistical scores is not very significative because of the small sample size.

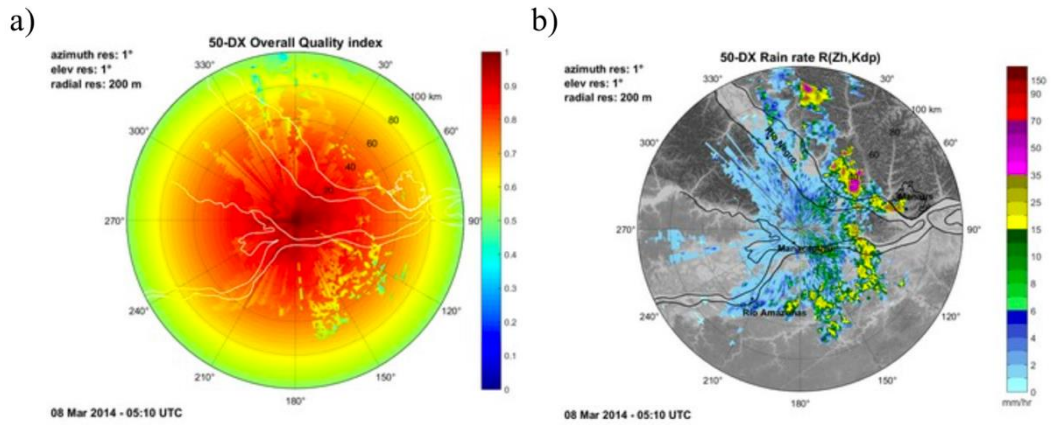


Figure 12 - a) Overall quality index radar on and b) Rain rate from radar on 08/03/2014 at 05:10UTC.

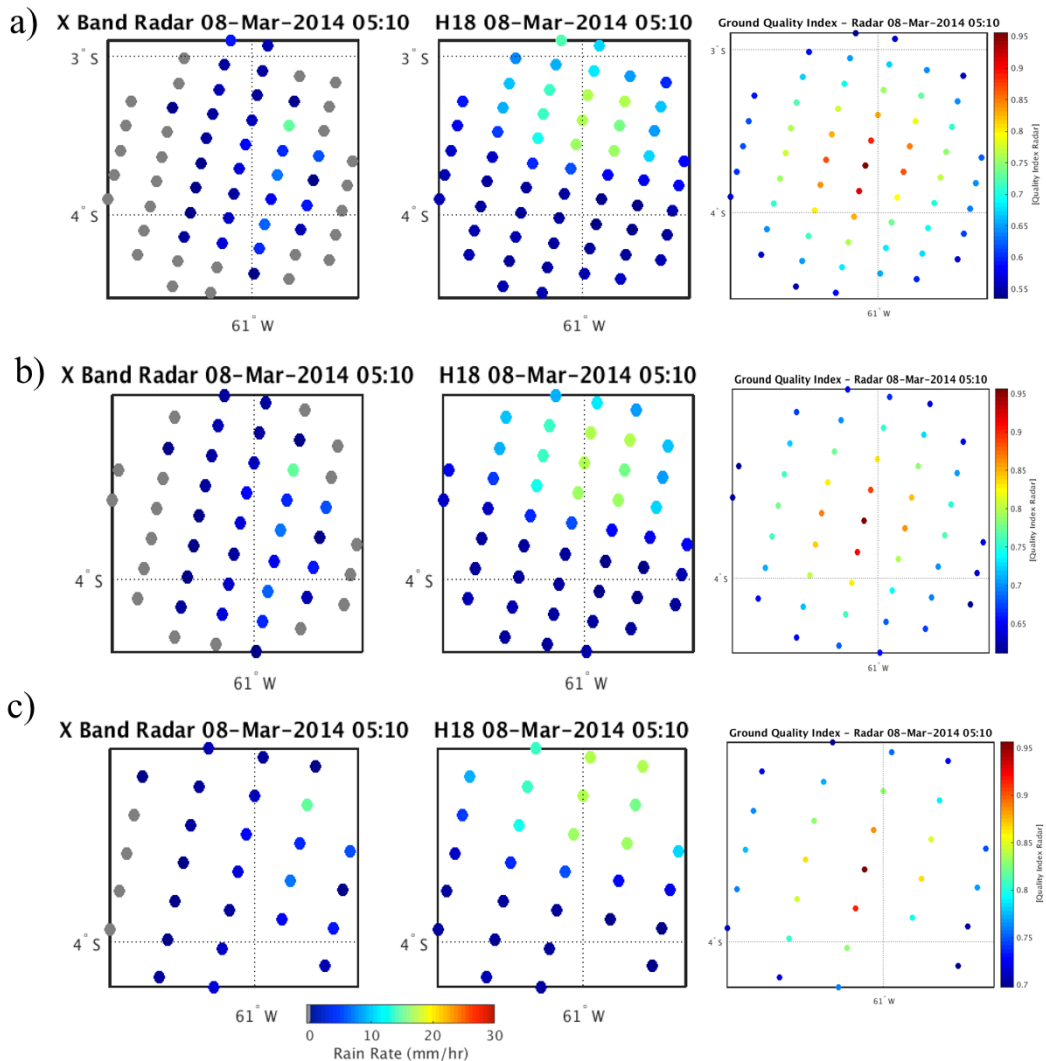


Figure 13 – Rain rate from radar upscaled to the satellite grid (left), H18 rain rate (center) and overall quality index map (right) in Manaus on 08/03/2014 at 05:10 for a) quality index > 0,5, b) quality index > 0,6 and c) quality index > 0,7.

The first example for Vale do Paraíba campaign is referred to the presence of convective clusters associated with the ZCAS (South Atlantic Convergence Zone). The matching between radar and satellite is occurred at 21:18UTC and depicts the presence of few intense convective cells close to the radar center with maximum rain rate between 50 and 70 mm/h (Fig. 14b). The overall quality index (Fig. 14a) on this region is mostly affected by the presence of beam blockage by two mountains chain, the Serra da Mantiqueira (on the West) and Serra do Mar (on the East). By analyzing the upscaled maps (Fig. 15) it is clear that, as opposed to Manaus, the precipitation pattern is well detected by H01. Concerning the rainfall rate estimates, for this case, the tendency of H01 is to underestimate the highest rainfall rates, while for the rest it is quite close to the reference, confirming what was shown with the statistical scores (ME close to zero).

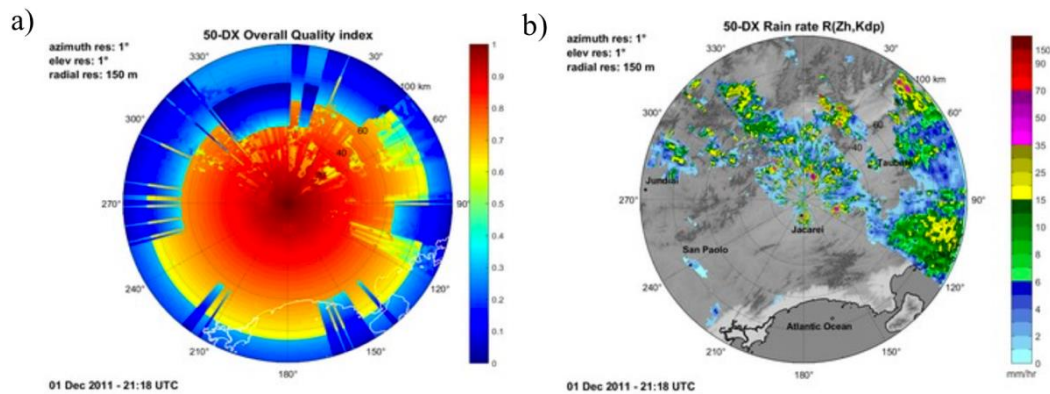


Figure 14 - a) Overall quality index radar on and b) Rain rate from radar on 01/12/2011 at 21:18UTC.

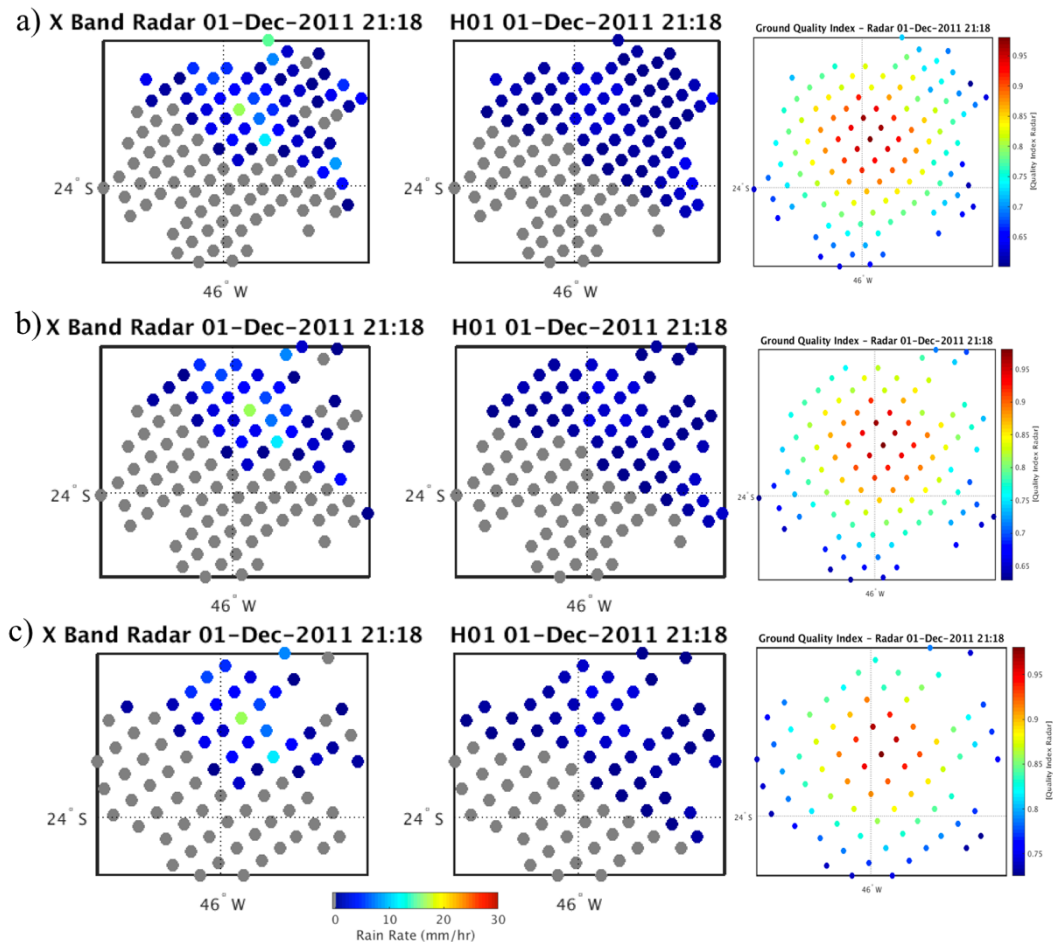


Figure 15 – Rain rate from radar upsampled to the satellite grid (left), H01 rain rate (center) and overall quality index map (right) in vale do Paraíba on 01/12/2011 at 21:18 for a) quality index > 0,5, b) quality index > 0,6 and c) quality index > 0,7.

The second example for Vale do Paraíba campaign shown in Fig. 16 and 17 for H02, refers to the presence of local convection with sparse intense convective cells occurring predominantly in the afternoon through the evening. The most intense convective cells shows the radar rainfall rates up to 70 mm/h. For this event, the pattern of the precipitation is also quite similar to the ground-based reference, which is also reflected by the lowest FAR values for H02 (in comparison to the other products). Also in terms of rainfall rate estimates, H02 is close to the radar, including the larger rain rates (light blue). The statistical scores shows low mean error values over this region for H02, suggesting a better detection and estimation over this region compared to Amazon region.

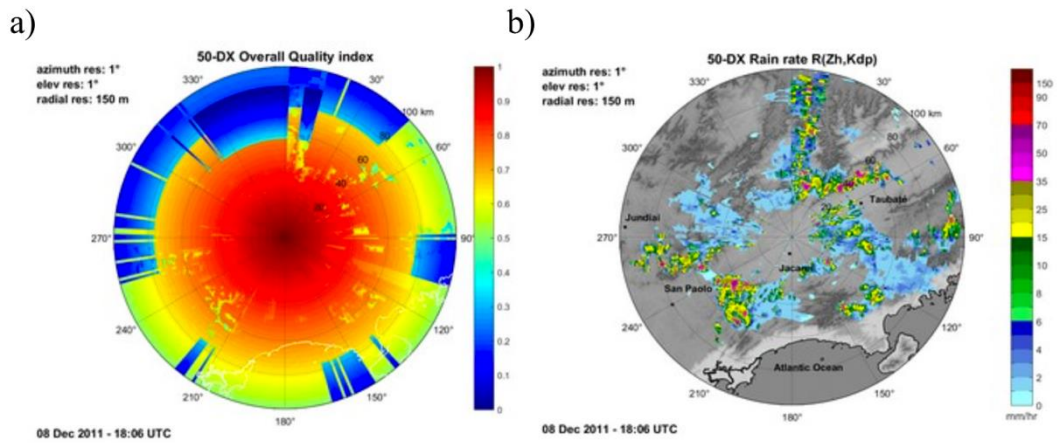


Figure 16 - a) Overall quality index radar on and b) Rain rate from radar on 08/12/2011 at 18:06UTC.

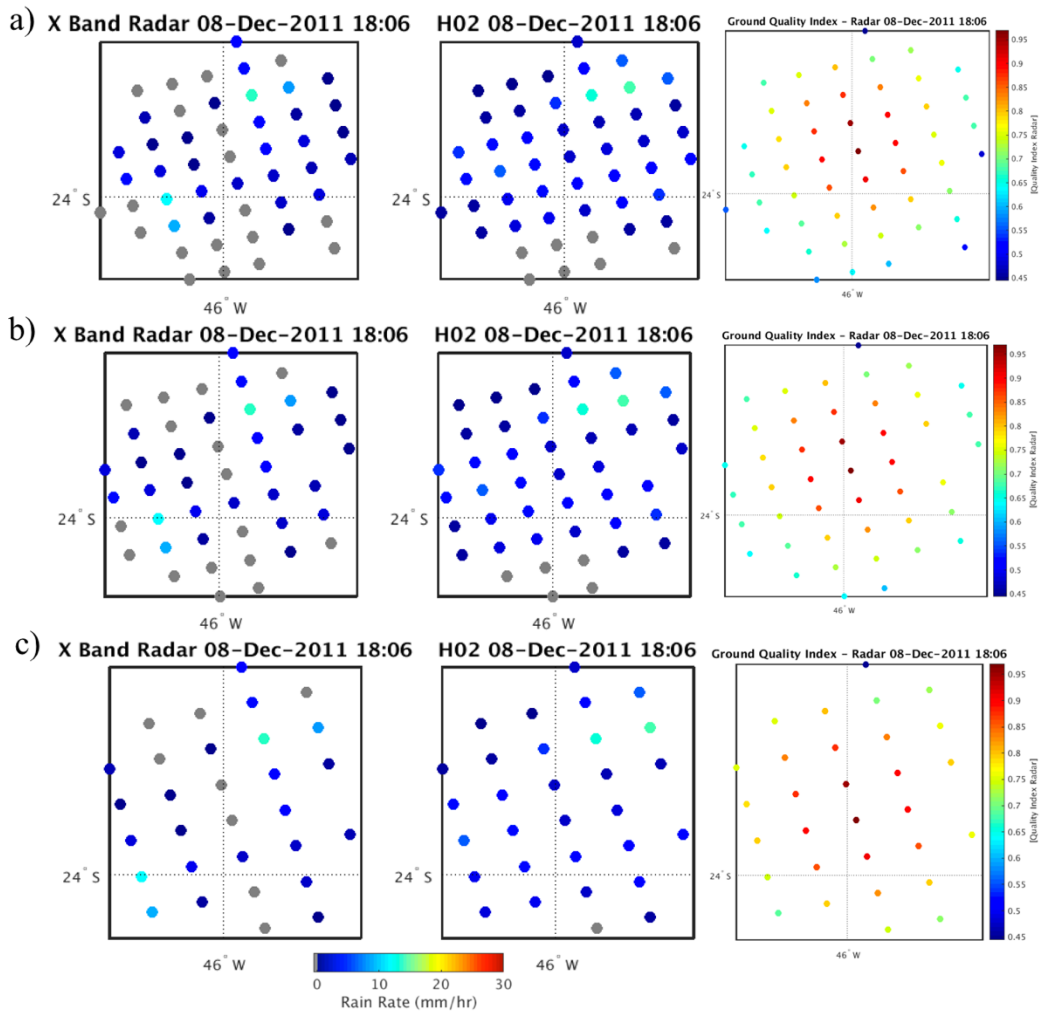


Figure 16 – Rain rate from radar upsampled to the satellite grid (left), H02 rain rate (center) and overall quality index map (right) on 08/12/2011 at 18:06 for a) quality index > 0,5, b) quality index > 0,6 and c) quality index > 0,7

## 7. CONSIDERATIONS AND CONCLUSIONS:

From the analysis showed above, it is possible to summarize the main aspects extracted from each product for the studied regions and provide suggestions for future improvements. The sample size, in all cases, was quite small and new verifications should be carried out over a larger and more comprehensive sample.

### 1) Manaus:

- H01 tends to have improvement on the statistical scores with increasing quality index, however tends to overestimate the light and heavy rain rate classes;

- H02 did not show improvements with the increase of quality index, presents better POD than H01, but also presents high FAR values.

- H18 presents lower overestimation of heavy rain rates compared to H02, probably due the different neural network used in H18.

In general, all algorithms showed high FAR values and larger areas of precipitation than the reference, due to the precipitation screening procedure which apparently is substantially affected by the high water vapor content on the Amazon region. Moreover, the variability of the surface in the region, is not represented in the *a priori* (or training) database used in the retrieval algorithms, while it is associated to “coastal area”, therefore subject to larger uncertainty in the retrieval.

### 2) Vale do Paraíba:

- Both algorithms, H01 and H02, produce mean error values quite close to zero (or negative) and lower FAR values (from 0,21 to 0,49) than Manaus. Differently from Manaus the precipitation patterns are well reproduced and the estimations are close to the reference. The analysis carried out on Vale do Paraíba and Manaus, indicates pathways for future development and studies. It is suggested to:

1) Perform new validations using a larger and more comprehensive sample of reference data for the Brazilian regions.

2) To improve the precipitation screening in order to better represent distinct regions (as the Amazon region).

3) To improve the surface classification in order to reduce the misclassification impact on the retrieval process.

4) Create a *a-priori* (or training) database representative of the distinct and typical precipitating systems in Brazil.

## 8. REFERENCES

Calheiros, A. J. P., and L. A. T. Machado, 2014: Cloud and rain liquid water statistics in the CHUVA campaign. *Atmos. Res.*, 144, 126–140, doi:10.1016/j.atmosres.2014.03.006.

Casella, D., Panegrossi, G., Sanò, P., Mugnai, A., Smith, E. A., Tripoli, G. J., Dietrich, S., Formenton, M., Leung, W. Y., and Mehta, A.: Transitioning from CRD to CDRD in bayesian re-trieval of rainfall from satellite passive microwave measure-ments: Part 2. Overcoming database profile selection ambiguity ity by consideration of meteorological control on microphysics, *IEEE T. Geosci. Remote*, 51, 4650–4671, 2013.

Machado, L. A. T. et al.. The CHUVA Project - how does convection vary across Brazil?.*Bulletin of the American Meteorological Society*, v. 95, p. 1-10, 2014.

Mugnai, A., Casella, D., Cattani, E., Dietrich, S., Laviola, S., Lev-izzani, V., Panegrossi, G., Petracca, M., Sanò, P., Di Paola, F., Biron, D., De Leonibus, L., Melfi, D., Rosci, P., Vocino, A., Zauli, F., Pagliara, P., Puca, S., Rinollo, A., Milani, L., Porcù, F., and Gattari, F.: Precipitation products from the hy-drology SAF, *Nat. Hazards Earth Syst. Sci.*, 13, 1959–1981, doi:10.5194/nhess-13-1959-2013, 2013a.

Mugnai, A., Smith, E. A., Tripoli, G. J., Bizzarri, B., Casella, D., Dietrich, S., Di Paola, F., Panegrossi, G., and Sanò, P.: CDRD and PNPR satellite passive microwave precipitation re-trieval algorithms: EuroTRMM/EURAINSAT origins and H- SAF operations, *Nat. Hazards Earth Syst. Sci.*, 13, 887–912, doi:10.5194/nhess-13-887-2013b.

Panegrossi, G., Casella, D., Dietrich, S., Marra, A. C., Milani, L., Petracca, M., Sanò, P., and Mugnai, A.: CDRD and PNPR pas-sive microwave precipitation retrieval algorithms: extension to the MSG full disk area, *Proc. 2014 EUMETSAT Meteorological Satellite Conference*, Geneva, [https://www.eumetsat.int/website/home/News/ConferencesandEvents/DAT\\_2076129.html](https://www.eumetsat.int/website/home/News/ConferencesandEvents/DAT_2076129.html), 2014.

Puca, S., Porcu, F., Rinollo, A., Vulpiani, G., Baguis, P., Balabanova, S., Campione, E., Ertürk, A., Gabellani, S., Iwanski, R., Jurašek, M., Kanák, J., Kerényi, J., Koshinchanov, G., Kozinarova, G., Krahe, P., Lapeta, B., Lábó, E., Milani, L., Okon, L., Öztopal, A., Pagliara, P., Pignone, F., Rachimow, C., Rebora, N., Roulin, E., Sönmez, I., Toniazzo, A., Biron, D., Casella, D., Cattani, E., Dietrich, S., Di Paola, F., Laviola, S., Levizzani, V., Melfi, D., Mugnai, A., Panegrossi, G., Petracca, M., Sanò, P., Zauli, F., Rosci, P., De Leonibus, L., Agosta, E., and Gattari, F.: The validation service of the hydrological SAF geostationary and polar satellite precipitation products, *Nat. Hazards Earth Syst. Sci.*, 14, 871–889, doi:10.5194/nhess-14-871-2014, 2014.

Rinollo, A., G. Vulpiani, S. Puca, P. Pagliara, J. Kaňák, E. Lábó, Ł. Okon, E. Roulin, P. Baguis, E. Cattani, S. Laviola, and V. Levizzani, 2013: Definition and impact of a quality index for radar-based reference measurements in the H-SAF precipitation product validation. *Nat. Hazards Earth Syst. Sci.*, 13, 2695-2705.

Sanò, P., Casella, D., Mugnai, A., Schiavon, G., Smith, E. A., and Tripoli, G. J.: Transitioning from CRD to CDRD in bayesian retrieval of rainfall from satellite passive microwave measurements: Part 1. Algorithm description and testing, *IEEE T. Geosci. Remote*, 51, 4119–4143, doi:10.1109/TGRS.2012.2227332, 2013.

Sanò, P., Panegrossi, G., Casella, D., Di Paola, F., Milani, L., Mugnai, A., Petracca, M., and Dietrich, S.: The Passive microwave Neural network Precipitation Retrieval (PNPR) algorithm for AMSU/MHS observations: description and application to European case studies, *Atmos. Meas. Tech.*, 8, 837–857, doi:10.5194/amt-8-837-2015, 2015.

Sanò, P., Panegrossi G., Casella, D., Marra, A. C., Paola, F.D., Dietrich, S..The new Passive microwave Neural network Precipitation Retrieval (PNPR) algorithm for the cross-track scanning ATMS radiometer: description and verification study over Europe and Africa using GPM and TRMM spaceborne radars, *Atmos. Meas. Tech.*, 9, 5441–5460, 2016.

Vulpiani, G., Baldini, L., and Roberto, N.: *Characterization of Mediterranean hail-bearing storms using an operational polarimetric X-band radar*, *Atmos. Meas. Tech.*, 8, 4681-4698, doi:10.5194/amt-8-4681-2015, 2015